

## ARTICLES

## Two-Photon Polymerization of Polydiacetylene

Olga Shusterman,<sup>†</sup> Amir Berman,<sup>‡,§</sup> Yuval Golan,<sup>§,||</sup> Baruch Horovitz,<sup>\*,†,§</sup> and Leila Zeiri<sup>§,⊥</sup>*Department of Physics, Department of Biotechnology Engineering, Ilse Katz Institute for Nanoscience and Nanotechnology, Department of Materials Engineering, and Department of Chemistry, Ben Gurion University of the Negev, Beer-Sheva 84105, Israel**Received: July 24, 2008; Revised Manuscript Received: September 14, 2008*

We show that visible light can polymerize diacetylene monomers into polydiacetylene (PDA) in a two-photon process. We monitor the process by measuring Raman intensities of PDA using a Raman laser at 633 nm with variable intensity  $I$  and show that the Raman cross section at short times increases as  $I^2$ , corresponding to a two-photon process. The process generates a relatively stable blue phase PDA, in contrast with UV polymerization that leads to a fast blue to red phase transformation.

## 1. Introduction

Polymerization of diacetylene into polydiacetylene (PDA) can be induced by UV light.<sup>1,2</sup> The process first leads to a so-called “blue” phase, while further UV light changes the blue phase into a “red” phase, and eventually the PDA degrades.<sup>3</sup> The kinetics of these processes have been studied in detail by following the characteristic absorption of the respective phases in the visible range.<sup>3–5</sup> Various studies used Raman spectra to follow the polymerization and the transitions between the different phases. Each phase exhibits a typical Raman spectra, and the kinetics is extracted from the changes of the different bands. The polymerization was induced by UV light<sup>6,7</sup> or  $\gamma$  radiation.<sup>8</sup> Polymerization of PDA by visible laser light followed by the Raman spectra has been reported for Langmuir–Blodgett films on rough silver surfaces.<sup>9,10</sup> A comprehensive study of the kinetic for different silver surfaces and different temperatures was done and the kinetic parameters were extracted. The significance of surface roughness was shown as the process did not take place on a smooth surface.

The rough metallic surface is well-known to enhance surface reactions as it is strongly polarizable. In particular, surface-enhanced Raman scattering (SERS) is well studied.<sup>11</sup> Recently, it was found that a Langmuir–Blodgett film of PCDA on an Ag plate polymerizes to the blue phase under 633 nm radiation, while no red phase was formed within the time frame of the experiment.<sup>12</sup> The smooth Ag plate is considered to be a non-SERS-active substrate; in contrast, the SERS-active, roughened Ag plate leads to the full sequence of monomer to blue and then to the red phase.<sup>12</sup>

Enhanced photochemical processes on rough (or SERS active) silver surfaces are known also for other reactions of aromatic molecules<sup>13,14</sup> where a quadratic ( $I^2$ ) dependence of the initial

reaction rate on the laser intensity ( $I$ ) was found. It was attributed to a two-photon absorption process enhanced at rough silver surfaces.

In the present work, we demonstrate that visible light can polymerize PCDA even on an uncoated glass substrate at room temperature. We use the laser of the Raman system to monitor the Raman intensities at characteristic frequencies of PDA phases, while this laser also polymerizes the PCDA. The reaction kinetics, where  $M$  is the monomer density and  $B$  is the PDA blue phase density, is given by

$$\frac{dM}{dt} = -kI^p M$$

$$\frac{dB}{dt} = kI^p M - k'I^{p'} B \quad (1)$$

Here,  $k$  is the M to B reaction rate and the power  $p$  signifies the type of reaction, with  $p = 1$  a one-photon process,  $p = 2$  a two-photon process, etc.;  $k'$  is the blue to red phase reaction rate with a different  $p'$  process. In the present work, we show that the B phase is stable over a long time compared with the time for M to B, hence  $k'I^{p'} \ll kI^p$ . Furthermore, we focus on the short time regime where the signal is linear with time, i.e., before the M to B transition is saturated. In this regime,  $B = kM_0 I^p t$ , where  $M_0$  is the initial density of the monomer. The Raman intensity is proportional to  $I \cdot B$ , hence we expect a Raman intensity  $\sim I^{p+1}$ . (Note that refs 13 and 14 plot Raman intensities/ $I$  probing directly  $\sim I^p$ .)

## 2. Experimental Section

**2.1. Materials.** 10,12-Pentacosadiynoic acid, PCDA, ( $(\text{CH}_2)_{11}\text{C}\equiv\text{C}-\text{C}\equiv\text{C}(\text{CH}_2)_8\text{COOH}$ ), 97% HPLC (Fluka) was purified by dissolving in cyclohexane:chloroform 9:1 solution and filtrating through a 0.22  $\mu\text{m}$  PTFE filter. Solvents were purchased from Sigma and used as received.

**2.2. Sample Preparation.** Microscope glass cover slides were cleaned with methanol, acetone, and isopropanol in sequence and air-dried. Solution of 6 mM PCDA in cyclohex-

\* Corresponding author. E-mail: hbaruch@bgu.ac.il.

<sup>†</sup> Department of Physics.<sup>‡</sup> Department of Biotechnology Engineering.<sup>§</sup> Ilse Katz Institute for Nanoscience and Nanotechnology.<sup>||</sup> Department of Materials Engineering.<sup>⊥</sup> Department of Chemistry.

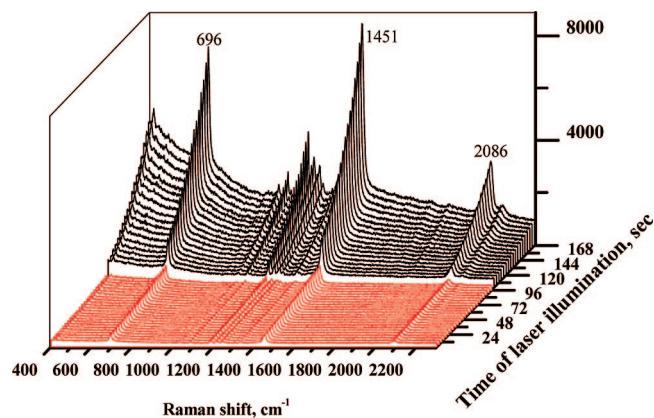


**Figure 1.** Micro-Raman spectra of PDA film on glass substrate as a function of the 633 nm irradiation time. Laser power was 3000 W/cm<sup>2</sup>. Calibration intensity was 1500 W/cm<sup>2</sup> during initial ~100 s. Similar raw data with all other intensities were used for Figure 2 and for Table 1.

ane:chloroform 9:1 was spin coated at 1000 rpm for 1 min to form a 100 nm thick film.

**2.3. Raman Characterization.** Raman spectra were collected using a Jobin-Yvon (JY) LabRam HR 800 micro-Raman system, equipped with a liquid-N<sub>2</sub>-cooled detector. Excitations were with 633 nm He–Ne laser or with 514 nm argon-green laser through a 50× microscope objective lens. The power on the sample was attenuated using neutral-density (ND) filters. Most measurements were taken using a 600 grooves/mm grating and a microscope confocal hole setting of 100 μm giving a resolution of about 4 cm<sup>-1</sup>.

### 3. Photopolymerization

Starting with PCDA monomers, we show the evolution of the Raman spectra with time in Figure 1, using a 633 nm Raman laser. The initial irradiation time of ~100 s was done with 1500 W/cm<sup>2</sup> intensity laser and serves as data calibration. Subsequent exposure was carried out at 3000 W/cm<sup>2</sup> intensity. This procedure was repeated with five different intensities, all with an initial intensity of 1500 W/cm<sup>2</sup> that was used to calibrate these five intensities. This initial calibration was needed since each intensity change was accompanied in a shift in position of the laser beam on the surface and hence probes a different spot on the sample. These spots may have a different thickness, and furthermore, the PDA domains at different spots may be differently oriented with respect to the polarized Raman light, leading to different scattering intensities. The integrated intensity of the characteristic triple bond line at 2086 cm<sup>-1</sup> is shown in Figure 2 as function of time. As expected from eq 1, the initial reaction rate is linear with time, while the slope is intensity dependent.

The various slopes of the three main Raman lines characteristic of the “blue” phase, 696, 1451, and 2086 cm<sup>-1</sup>, are presented in Table 1. The ratios of the 1500 W/cm<sup>2</sup> data are used as calibrations, so that below each number we present its calibrated value (see table caption for more detail). The row for 1500 W/cm<sup>2</sup> intensity uses the calibration data of the row for the 3000 W/cm<sup>2</sup> intensity. We note that the calibration slope associated with the 3000 W/cm<sup>2</sup> intensity is lower than the other slopes, which may indicate a smaller beam spot on the sample or a spot with incomplete coverage.

The normalized intensity slopes are shown in Figure 3 with fitted lines of  $I^{p+1}$ , where  $p + 1 = 2.90, 3.05, 3.06$  for the three Raman lines. We note that the calibration described above is

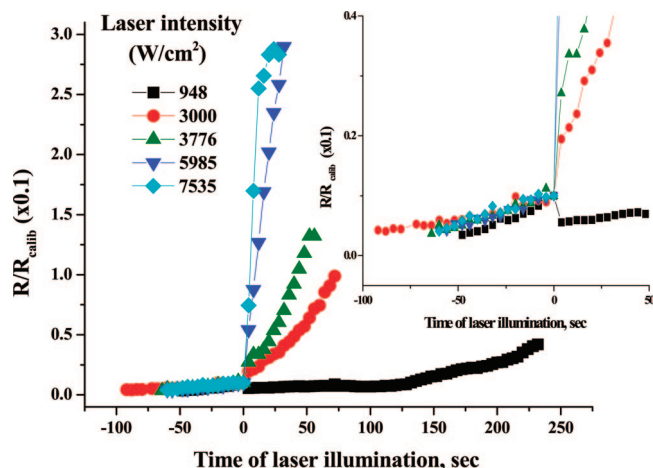


**Figure 2.** Dependence of the triple bond line intensity,  $R$ , at 2086 cm<sup>-1</sup> on time of laser illumination for various laser intensities  $I$  (in W/cm<sup>2</sup>). The scale is set by normalization of the observed intensities with respect to  $R_{\text{calib}}$ , the observed intensity at the end of the calibration stage. The initial 50–100 s for each measurement were taken at laser intensity of 1500 W/cm<sup>2</sup> and used for calibration. The maximum measured intensity was  $3.8 \times 10^4$  ( $I = 948$  W/cm<sup>2</sup>),  $5.2 \times 10^4$  ( $I = 3000$  W/cm<sup>2</sup>),  $1.5 \times 10^5$  ( $I = 3776$  W/cm<sup>2</sup>),  $3.25 \times 10^5$  ( $I = 5985$  W/cm<sup>2</sup>), and  $4.2 \times 10^5$  ( $I = 7535$  W/cm<sup>2</sup>); counts for the laser intensities indicated in parentheses. The inset shows a normalized expanded view of the calibration stage.

crucial for obtaining consistent fits. Figure 3 therefore proves our claim, i.e.,  $p = 2$  with a reasonably high accuracy. We conclude that indeed, in the visible range, a two-photon process can polymerize pure PCDA monomers also on nonmetallic substrates.

### 4. Blue to Red Transition

In Figure 4 we show Raman data after long exposure time of 633 nm at 1600 W/cm<sup>2</sup>. It is seen that the blue phase peaks reach a maximum value at ~60 s, then decrease by ~50%, and remain constant for at least 35 min; no peaks corresponding to the red phase are seen within the time scale in Figure 4. In contrast, the UV polymerization data in Figure 5 shows the blue phase peaks vanishing gradually within ~10 min, with the red phase peaks appearing instead; e.g., the double bond at 1456 cm<sup>-1</sup> (blue phase) is replaced by 1520 cm<sup>-1</sup> of the red phase. Notably, the PDA red phase is off-resonance when a 633 nm laser is used, hence the low intensity of the corresponding Raman line (2120 cm<sup>-1</sup>). We note that the triple bond at 2086 cm<sup>-1</sup> (blue phase) has a 2150 cm<sup>-1</sup> satellite within the blue phase; the proper red phase has its triple bond at 2120 cm<sup>-1</sup> (see also Figure 7).

In Figure 6 we show high-intensity data with  $I = 30\,000$  W/cm<sup>2</sup>, where the red phase double bond of 1520 cm<sup>-1</sup> is seen to appear already at 40 s, while the 1456 cm<sup>-1</sup> line of the blue phase is decreasing after ~2 min. The red phase Raman peaks are relatively weak since the 633 nm light is off-resonance from the red phase absorption at 550 nm. Yet, the weak signal of the red phase 1520 cm<sup>-1</sup> shows that the blue to red kinetics relative to the monomer to blue transition is much slower with the 633 nm laser than with the UV radiation, i.e.,  $kI' \ll kI^p$  for the 633 nm laser process.

In contrast, the data with 440 and 532 nm lasers shows that the blue to red transition<sup>9,15</sup> is readily induced. A possible interpretation is that with 532 nm or shorter wavelengths the blue to red is a one-photon transition, while with our 633 nm laser this transition is a two-photon process.

TABLE 1: Fitted Slopes of the Main Raman Lines 694, 1451, and 2086  $\text{cm}^{-1}$ <sup>a</sup>

intensity	Raman					
	696 $\text{cm}^{-1}$		1451 $\text{cm}^{-1}$		2086 $\text{cm}^{-1}$	
	1500 $\text{W}/\text{cm}^2$ calibration		1500 $\text{W}/\text{cm}^2$ calibration		1500 $\text{W}/\text{cm}^2$ calibration	
948 $\text{W}/\text{cm}^2$	188	52	316	111	120	48.7
	4.7	11	4	26.8	3.6	14
1500 $\text{W}/\text{cm}^2$		40		75.9		33.5
3000 $\text{W}/\text{cm}^2$	40	735	75.9	1361	33.5	604
	1	735	1	1361	1	604
3776 $\text{W}/\text{cm}^2$	174	2906	287	6245	119	2830
	4.3	670	3.8	1652	3.6	795
5985 $\text{W}/\text{cm}^2$	193	8344	272	20407	110	9405
	4.8	1733	3.6	5700	3.3	2885
7535 $\text{W}/\text{cm}^2$	192	27694	375	80804	148	32865
	4.8	5776	4.9	16390	4.4	7469

<sup>a</sup> The data analysis for 2086  $\text{cm}^{-1}$  is displayed in Figure 2. For each intensity the upper line displays the measured slopes: three columns (labeled with "calibration") list slopes of the Raman intensities with the calibrating intensity of 1500  $\text{W}/\text{cm}^2$  and three columns for the slopes of the Raman intensities with varying laser intensities, as listed on the left column. The lower line for each intensity displays calibrated slopes, obtained by dividing the data by the ratio of calibration data (e.g., for the 696 line at 948  $\text{W}/\text{cm}^2$  the ratio is  $188/40 = 4.7$ , hence the slope 52 is reduced to 11). The 1500  $\text{W}/\text{cm}^2$  row uses the calibration data of the 3000  $\text{W}/\text{cm}^2$  row as input data for the 1500  $\text{W}/\text{cm}^2$  row.

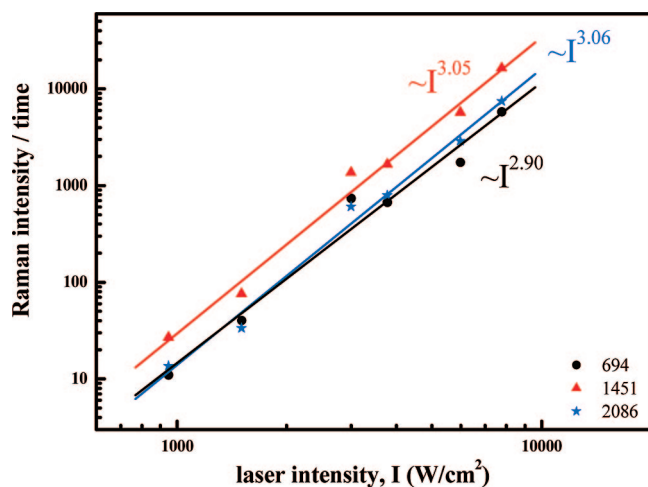


Figure 3. Dependence of normalized intensity slopes (straight line slopes of Figure 2 and numbers on lower lines of each intensity in Table 1) on laser intensity for different Raman shifts ( $\text{cm}^{-1}$ ).

To further study the blue to red transition, in Figure 7 we show that after a 140 min application of a 400  $\text{W}/\text{cm}^2$  laser of 633 nm, a 2 min application of a 514 nm laser readily induces a red phase component that is sensitive to the 514 nm probe. When switching back to a 633 nm laser, the blue phase peaks are similar to those before the application of the 514 nm laser within a few percent; i.e., the blue to red conversion has been small. The 514 nm light is in resonance with the red phase, hence it is sensitive even to these small concentrations of the red phase.

To conclude this section, we have shown that the blue to red conversion with 633 nm is much slower than the polymerization rate (Figure 4) and needs very high intensities to be observed (Figure 6). This is in contrast with a UV-induced process (Figure 5) or even a 514 nm light induced process (Figure 7), where the blue to red conversion is relatively fast. These observations lead us to propose that the blue to red conversion with 633 nm photons is also a 2-photon process. We have not done, however,

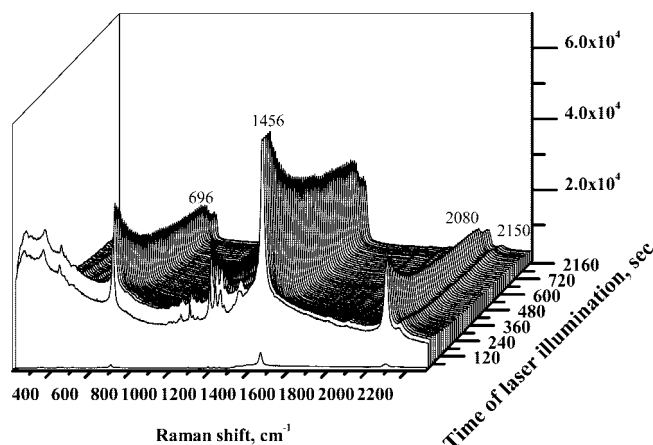
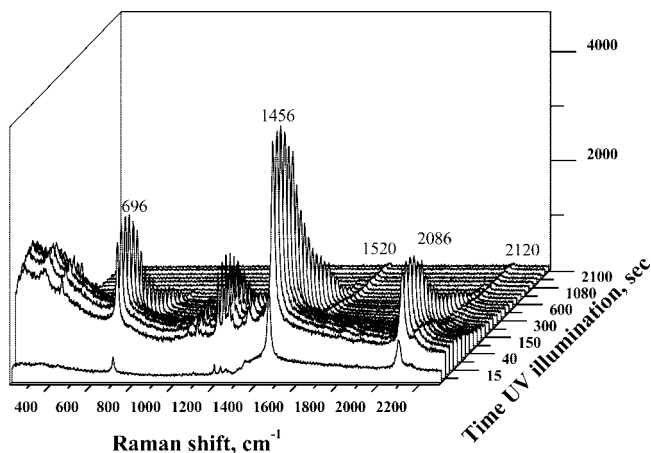


Figure 4. Micro-Raman spectra of PDA film on glass substrate as a function of the 633 nm irradiation time. Laser power was 1600  $\text{W}/\text{cm}^2$ . Note the change in scale beyond 720 s.

a quantitative analysis as we have for the photopolymerization in Figure 3. This is due to the limited range of available strong intensity lasers where this process can be quantified.

## 5. Discussion

Visible light is shown to induce photopolymerization in PDA films on glass substrates. The polymerization rate was found to depend on the laser intensity as  $I^2$ , leading to Raman scattering from PDA modes that correspondingly varies as  $I^3$ . The energy of two 633 nm photons correspond to a single 316 nm photon, fairly close to the 254 nm UV light commonly used for photopolymerization. We show then that two-photon excited states of the monomer lead to polymerization, similar to a single UV photon. This is the first demonstration that two-photon polymerization of PDA is feasible without a SERS-active surface on a glass substrate. We note that Joo et al.<sup>12</sup> showed photopolymerization on an Ag plate, which is considered to be a non-SERS-active substrate. While the effects of an Ag plate on photopolymerization are not obvious, our results obtained



**Figure 5.** Micro-Raman spectra of PDA film on glass substrate as a function of UV illumination time. 633 nm laser at 400 W/cm<sup>2</sup>, 254 nm UV lamp at  $24 \times 10^{-3}$  W/cm<sup>2</sup>.

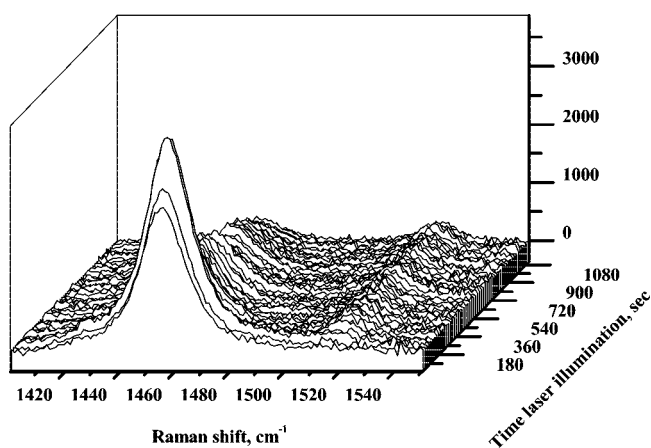


**Figure 6.** Micro-Raman spectra of double bond frequency of PDA film on glass substrate as a function of the 633 nm irradiation time. Laser power was 30 000 W/cm<sup>2</sup>.

on glass substrate provide unequivocal proof that the photopolymerization is intrinsic to the PCDA and in particular that it is a two-photon process.

Furthermore, we have also found that the blue to red transition is extremely weak under these conditions, in contrast to the common photopolymerization done with UV light. Since this process has been shown to occur with 440 nm light,<sup>14</sup> we conclude that the energy of a single 633 nm photon, though well within the absorption of the blue phase, is not sufficiently energetic to induce a blue to red transition, hence supporting our conclusion that this transition is likely to be a two-photon process.

We note also that with 532 nm light and a SERS-active surface the blue to red transition is faster than the polymerization,<sup>9,10</sup> the SERS condition is essential for this observation. In contrast, the glass surface allows polymerization with 633 nm light, stabilizing a fairly pure blue phase; this blue phase is stable for  $\sim 10$  times longer than the time for photopolymerization. In contrast to our kinetics analysis of UV-induced polymerization and phase transformation<sup>4</sup> that show that the under those conditions the blue phase always coexists with the monomer and red phase PDA polymer, here we show that almost pure

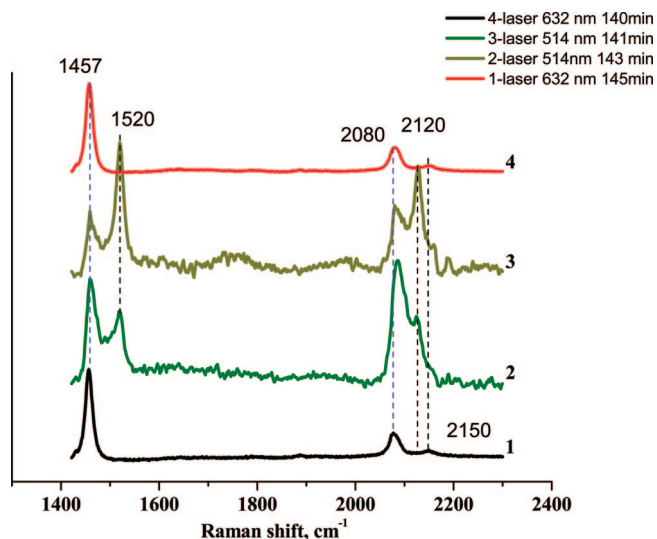


**Figure 7.** Micro-Raman spectra of PDA film on glass substrate as a function of the 633 and 514 nm irradiation time. Laser power was 400 W/cm<sup>2</sup> at 633 nm and 452 W/cm<sup>2</sup> at 514 nm (note that the 2086 cm<sup>-1</sup> line shifts somewhat in the polymerization process and appears here as 2080 cm<sup>-1</sup>).

PDA blue phase can be produced on glass by 2-photon process at 633 nm wavelength.

**Acknowledgment.** We thank V. Vardeny for illuminating discussions and useful comments. We also thank A. Vilan for help and useful discussions. This work was supported by the German-Israeli Foundation for Scientific Research and Development (grant G-791-133.10/2003).

## References and Notes

- (1) Tieke, B.; Wegner, G.; Naegel, D.; Ringsdorf, H. *Angew. Chem., Int. Ed. Engl.* **1976**, *15*, 704.
- (2) Carpick, R. W.; Sasaki, D. Y.; Marcus, M. S.; Eriksson, M. A.; Burns, A. R. *J. Phys.: Condens Matter* **2004**, *16*, R679.
- (3) Lifshitz, Y.; Upcher, A.; Shusterman, O.; Horovitz, B.; Berman, A.; Golan, Y. Submitted for publication in *J. Phys. Chem. B*.
- (4) Hofmann, U. G.; Peltonen, J. *Langmuir* **2001**, *17*, 1518.
- (5) Koshihara, S.; Tokura, Y.; Takeda, K.; Koda, T. *Phys. Rev. B: Condens. Matter* **1995**, *52*, 6265.
- (6) Shirai, E.; Urai, Y.; Itoh, K. *J. Phys. Chem. B* **1998**, *102*, 3765.
- (7) Lazareva, O. L.; Schengolikhin, A. N. *Synth. Met.* **1997**, *84*, 991.
- (8) Schengolikhin, A. N.; Lazareva, O. L. *Spectrochim. Acta A* **1997**, *53*, 67.
- (9) Itoh, K.; Nishizawa, T.; Yamagata, J.; Fujii, M.; Osaka, N.; Kudryashov, I. *J. Phys. Chem. B* **2005**, *109*, 264.
- (10) Itoh, K.; Kudryashov, I.; Yamagata, J.; Nishizawa, T.; Fujii, M.; Osaka, N. *J. Phys. Chem. B* **2005**, *109*, 271.
- (11) For a review on SERS see: Moskovits, M. *Rev. Mod. Phys.* **1985**, *57*, 783.
- (12) Joo, S.-W.; Lim, J. K.; Cho, K. *J. Photochem. A* **2008**, *194*, 356.
- (13) Goncher, G. M.; Parsons, C. A.; Harris, C. B. *J. Phys. Chem.* **1984**, *88*, 4200.
- (14) Wolkow, R. A.; Moskovits, M. *J. Chem. Phys.* **1987**, *87*, 5858.
- (15) Ishikawa, K.; Fukagai, K.; Kanetake, T.; Koda, T.; Tokura, Y.; Koshihara, S. *Synth. Met.* **1989**, *28*, D605.